Cytometry
PART A
Journal of the International Society for Advancement of Cytometry

Multiplexed Labeling of Viable Cells for High-Throughput Analysis of Glycine Receptor Function Using Flow Cytometry

Daniel F. Gilbert,[1] John C. Wilson,[1] Virginia Nink,[1] Joseph W. Lynch,[1,2] Geoffrey W. Osborne[1,3]*

[1]Queensland Brain Institute, University of Queensland, Brisbane QLD 4072, Australia

[2]School of Biomedical Sciences, University of Queensland, Brisbane QLD 4072, Australia

[3]The Australian Institute for Bioengineering and Nanotechnology, University of Queensland, Brisbane QLD 4072, Australia

Received 16 October 2008; Revision Received 28 November 2008; Accepted 18 December 2008

Grant sponsor: National Health and Medical Research Council of Australia.

*Correspondence to: Geoffrey Osborne, Queensland Brain Institute, University of Queensland, Brisbane QLD 4072, Australia.

Email: g.osborne@uq.edu.au

Published online 30 January 2009 in Wiley InterScience (www.interscience.wiley.com)

DOI: 10.1002/cyto.a.20703

Abstract

Flow cytometry is an important drug discovery tool because it permits high-content multiparameter analysis of individual cells. A new method dramatically enhanced screening throughput by multiplexing many discrete fixed cell populations; however, this method is not suited to assays requiring functional cellular responses. HEK293 cells were transfected with unique mutant glycine receptors. Mutant receptor expression was confirmed by coexpression of yellow fluorescent protein (YFP). Commercially available cell-permeant dyes were used to label each glycine receptor expressing mutant with a unique optical code. All encoded cell lines were combined in a single tube and analyzed on a flow cytometer simultaneously before and after the addition of glycine receptor agonist. We decoded multiplexed cells that expressed functionally distinct glycine receptor chloride channels and analyzed responses to glycine in terms of chloride-sensitive YFP expression. Here, data provided by flow cytometry can be used to discriminate between functional and nonfunctional mutations in the glycine receptor, a process accelerated by the use of multiplexing. Further, this data correlates to data generated using a microscopy-based technique. The present study demonstrates multiplexed labeling of live cells, to enable cell populations to be subject to further cell culture and experimentation, and compares the results with those obtained using live cell microscopy. © 2009 International Society for Advancement of Cytometry

Key terms

multiplex; chloride channels; glycine receptor

FLOW cytometry permits multiple cell parameters to be analyzed simultaneously with high sensitivity and a high degree of statistical robustness. It is emerging as an important drug discovery tool because it can screen test compounds against a wide variety of cellular targets simultaneously. However, achieving this goal is dependant on two factors: (1) the ability to automate the screening of large numbers of compounds, and (2) the ability to monitor multiple parameters simultaneously in live cells. Recent developments (reviewed by Sklar et al. (1)), while useful, require dedicated hardware on an unmodified flow cytometer.

Multiplexed or duplexed analysis allows the screening of multiple discrete samples in one tube or well at the same time (2–4). A recent method (5), which introduced the idea of labeling discrete cell populations with a unique combination of fluorochromes, demonstrated the feasibility of employing flow cytometry to discriminate between different multiplexed labeled cell populations. However, this method required cellular fixation, preventing further culture or experimentation.

Glycine receptors (GlyRs) are pentameric Cys-loop anion-permeant channels that mediate inhibitory neurotransmission in the spinal cord, brainstem, and retina (6,7). These receptors have recently emerged as therapeutic targets for chronic inflammatory pain and movement disorders (8–10). Our interest lies in discovering novel bioactive compounds with therapeutic potential and in identifying mutations

ISAC
International Society for Advancement of Cytometry

within GlyRs that may reveal the binding sites of such compounds. The later project involves screening a large random mutant library for mutant clones that alter GlyR pharmacological properties. Because GlyR activation gates a Cl^- influx, its activation can be monitored using yellow fluorescent protein (YFP) variants that are highly sensitive to quenching by small anions and are thus suited to reporting anionic influx into cells (11,12). Currently, fluorescence quenching of adherent cells in response to agonist is assessed using a specialized imaging microscope plate-based system. This system, while effective, is limited by the number of cells that can be analyzed and by the number of parameters that can be monitored simultaneously.

The aim of this study was to establish a sensitive multiplexed flow cytometry method that would permit the rapid assessment of pooled sample responses to identical stimuli. This could, for example, permit multiple mutant clones to be screened simultaneously, or allow individual test compounds to be screened against multiple ion channel isoforms (not necessarily all GlyRs) simultaneously. Here, we describe an assay to label multiple live cell populations in a multiplexed manner. The GlyR agonist concentration-responses reported by this system are comparable with those generated with a conventional microscopy-based detection system. Importantly, we show that this technique is capable of increasing throughput by a factor of 12, although future developments should increase this factor even more. In addition, this approach provides additional time-related information that may be valuable in the characterization of different labeled cell populations. Finally, this assay is suited to any site with access to a multilaser flow cytometer and an interest in low cost, high-throughput screening of live cells.

Materials and Methods

Molecular Constructs

The GlyR cDNAs used in this study were the human α1 subunit in the pCIS2 plasmid vector and the human α2 and α3L subunits in the pcDNA3.1 plasmid vector. The following α1 GlyR mutants (also in the pCIS2 plasmid vector) were also employed: F63A; R65K; E103C; K104C; S129V; K200R; R271C; and R271Q. This range of wild type and mutant GlyRs was chosen as their glycine EC_{50} values are spread evenly over more than two orders of magnitude (13–16) and thus should allow the discriminatory capacity of the multiplex assay to be clearly validated. We also used the YFP-I152L mutant cDNA in the pcDNA3.1 vector as the sensor for GlyR activation. GlyR activation was quantitated by monitoring the fluorescence emission intensity of YFP-I152L, which is potently quenched by iodide ions (11). These anions permeate efficiently into the cell through activated GlyRs (12). We have previously shown that this YFP-I152L fluorescence quench is potently antagonized by the GlyR-specific antagonists, picrotoxin and strychnine (12).

Cell Culture and Transfection

All experiments were performed on HEK293 cells cultured in Dulbecco's Modified Eagle Medium (DMEM) supplemented with 10% fetal calf serum and 1% penicillin/streptomycin. Cells were maintained in a humidified 5% CO_2 atmosphere at 37°C and passaged weekly. Cells were cultured in 60-mm tissue culture dishes that were each seeded with 5 ml of cells at a density of 2×10^6 cells ml^{-1}. When 40–80% confluent, they were transfected with 0.5 μg of plasmid cDNA encoding YFP-I152L and 0.5 μg of GlyR cDNA using a standard calcium phosphate coprecipitation protocol (17). Transfection was terminated after 12–24 h by washing the cells twice in divalent cation-free phosphate buffered saline (PBS).

The cells were then trypsinized (0.25% Trypsin-EDTA, Gibco 25200-056), resuspended into DMEM, and counted. 2.5×10^3 cells were plated into each well of a transparent 384-well plate (BD). Cells were used in experiments 24–36 h after this procedure.

Imaging of Adherent Cells with the Custom Conventional Imaging System

Approximately 1 h before commencement of experiments, culture media in 384-well plates was removed from the cells and replaced by 25 μl standard control solution, containing (in mM): NaCl 140, KCl 5, $CaCl_2$ 2, $MgCl_2$ 1, HEPES 10, glucose 10, pH 7.4 using NaOH.

The 384-well plates were placed onto a motorized stage (Prior ProScan II) of an Olympus IX51 inverted microscope and cells were imaged with an Olympus 10× objective (UPlanFLN, N.A. 0.30). Illumination was from an Osram 100 W mercury short arc lamp (HBO 103/2), passing through an Olympus YFP dichroic mirror (86002V2 JP4 C76444), excited YFP fluorescence. Emitted fluorescence passed through a magnifier lens (diopter 8, mineral glass) was imaged by an Olympus CCD camera (CoolSNAP monochrome cf/OL) then digitized onto a personal computer. The final resolution of cell images was 696 × 520 pixels. The maximum image acquisition rate was 1.25 Hz. Liquid-handling was performed with an LC PAL autosampler (CTC Analytics) using a 100 μl syringe. A suite of LabView 7.1 and 8.2.1 software (National Instruments) routines purpose-written in the laboratory were used for hardware control, image acquisition, storage, image analysis, and data quantification. Experimental protocol involved imaging each well twice: once in 25 μl control solution and once again 8 s after the injection of 50 μl NaI test solution. Individual dose-responses were constructed by pooling results from two wells exposed to different test solutions containing the same glycine concentration. Each image typically contained 400–600 cells with sufficient fluorescence to be used for analysis. Experiments were replicated at least three times using cells from different passages transfected on different days.

Flow Cytometry Reagents

The cell-permeant fluorochromes used were Celltrace Calcein Blue AM (C34853), Celltrace Calcein Violet AM (C34858), and Celltrace Far Red DDAO-SE (C34553), which were obtained from Molecular Probes. All cell-permeant fluorochromes were brought to room temperature before opening. Forty-two microliters of DMSO (Sigma) was added to 25 μg of Celltrace desiccate and mixed vigorously. A working

Table 1. Comparison of glycine EC_{50} and n_H values for the indicated GlyR constructs measured using the two systems

	IMAGING SYSTEM		FLOW CYTOMETRY	
GlyR	EC_{50} (μM)	n_H	EC_{50} (μM)	n_H
α1	24 ± 4	1.2 ± 0.2	23 ± 5	3.8 ± 2.9
α2	23 ± 4	3.5 ± 1.9	24 ± 5	1.4 ± 0.3
α3	22 ± 4	2.1 ± 0.9	23 ± 3	1.6 ± 0.3
α1K200R	1,197 ± 67	2.4 ± 0.3	1,554 ± 145	1.9 ± 0.3
α1R65K	2,641 ± 142	2.7 ± 0.5	2,887 ± 131	3.1 ± 0.8
α1K104C	45 ± 19	1.2 ± 0.6	27 ± 15	0.7 ± 0.3
α1E103C	1,467 ± 348	1.1 ± 0.3	945 ± 406	1.9 ± 1.5
α1R271C	595 ± 67	1.2 ± 0.1	477 ± 66	1.7 ± 0.3
α1S129V	2,861 ± 165	1.9 ± 0.2	3,111 ± 765	1.2 ± 0.3
α1F63A	14,480 ± 2,700	5.0 ± 2.4	12,550 ± 2,540	3.2 ± 2.1

solution was prepared by adding 1.25 ml of PBS to 40 μl of Celltrace/DMSO solution and mixed vigorously; however, PBS was only added immediately before staining cells.

Multiplex Staining

All cell populations to be multiplexed were placed in 96-well U bottom plates at 100–250 × 10^3 cells/well and centrifuged at 300*g* for 5 min. Working solutions of fluorochromes were added (Calcein Blue 10 μl; Calcein Violet 10 μl; DDAO 0.4 μl (low stain) or 10 μl (high stain)) and each tube was made up to 50 μl with PBS if required. Fluorochromes were added as required to each cell population (see Fig. 5a) and each dye was triturated several times for adequate mixing. The stained cells were incubated at room temperature for 20 min, wrapped in aluminum foil, and placed on a MS-1 Minishaker (IKA) at 800 revolutions/minute. After incubation, cells were washed in 200 μl of control solution and centrifuged at 300*g* for 5 min after which supernatant was aspirated and the washing step repeated twice more. After the final wash, cells were resuspended in 200 μl of control solution.

Flow Cytometry

Samples were analyzed on a BD Biosciences LSR II, with four laser sources: violet (405 nm), blue (488 nm), and red (633 nm) all 20 at mW laser power, and UV (355 nm) at 50 mW laser power. Fluorescence collection filters used were YFP (530/30BP), compensation parameter (660/20BP), DDAO (660/20BP), Calcein Violet (450/50BP), and Calcein Blue (450/50BP). A 100 μl sample from each of the wells to be multiplexed was added to a single 5 ml polystyrene round bottom Falcon tube. This multiplex tube was centrifuged at 300*g* for 5 min, after which the supernatant was removed and the cells resuspended in 200 μl of control solution. The multiplexed cells were then split into two tubes (100 μl into each tube), with the first "control" tube having an additional 200 μl of control solution added, while the second tube had 200 μl of NaI solution containing 1.5 mM glycine added. The tubes were run immediately (within 10 s) on the flow cytometer. For both tubes, ~10 × 10^3 events per multiplexed cell population were analyzed using FCS Express 3 (De Novo Software, USA) software. In the glycine concentration-response experiments (results summarized in Table 1), 200 μl of glycine solution of varying concentrations was added to 100 μl of cells (not multiplexed) and each tube was analyzed on the flow cytometer immediately after the addition of glycine.

Statistical Analysis

Glycine concentration-response curves were fitted with the following equation:

$$F = F_{\text{init}} / \left(1 + (\text{EC}_{50}/[\text{glycine}])^{n\text{H}}\right)$$

where F is the fluorescence corresponding to a given glycine concentration, [glycine], F_{init} is the initial (or control) fluorescence value, EC_{50} is the glycine concentration that elicits a half-maximal response, and n_H is the Hill coefficient. Curve fits were performed using a least-squares fitting routine (Origin 7, OriginLab Corporation). All averaged experimental results are expressed as mean ± SEM. Statistical significance was determined by paired or unpaired Student's *t*-test, as appropriate, with $P < 0.05$ representing significance.

Results

Detection of YFP Quench by Flow Cytometry and Fluorescence Imaging

Sample images of HEK293 cells transfected with both YFP-I152L and the GlyR α1 subunit using the conventional imaging system are shown in Figure 1a. Images in the top row were recorded with cells exposed to the NaCl control solution. The corresponding images in the bottom row were taken 8 s after this solution was replaced by either control NaI solution alone (left) or NaI + 1 mM glycine (right). NaI is used in test solutions as I^- quenches fluorescence much more efficiently than Cl^- (9). To quantify the change in fluorescence after the addition of NaI + 1 mM glycine, the fluorescence of individual cells in control solution was plotted against the fluorescence following replacement by the test (NaI or NaI + glycine) solution (Fig. 1b, left). This graph confirms the trend, apparent in Figure 1a, that virtually all cells are quenched following the addition of NaI + glycine. These data are plotted in histogram form in Figure 1b (right panel). Percentage fluorescence change was defined as $((F_{\text{final}}/F_{\text{init}}) - 1) \times 100$ where F_{init} and

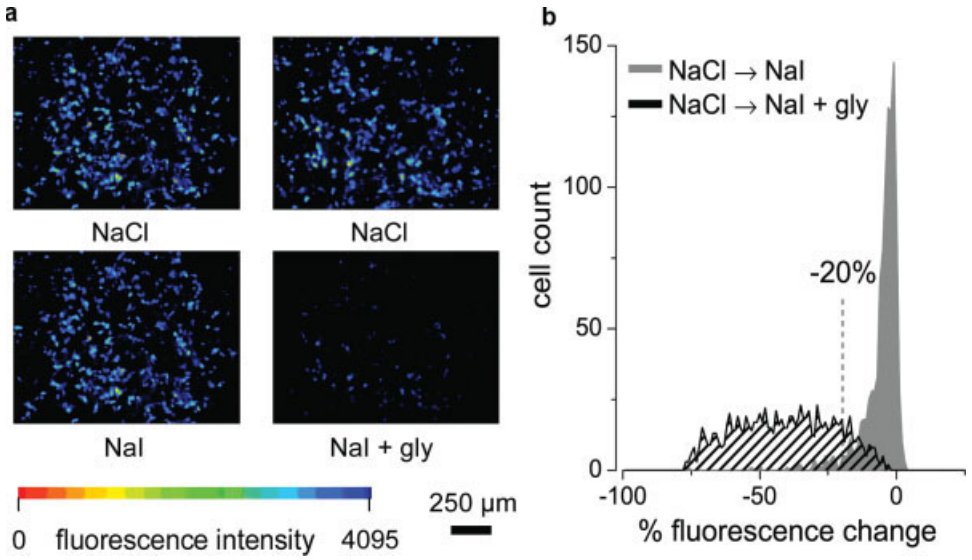

Figure 1. Response characteristics of cells expressing YFP-I152L and the α1 GlyR subunit imaged with the conventional imaging system. (**a**) Images in the upper row were recorded in the presence of NaCl control solution whereas the corresponding images in the lower row were recorded from the same well 8 s after replacement with either NaI alone (left image) or NaI + 1 mM glycine (right image). All images were recorded from the same 384-well plate, which had a mean YFP expression efficiency of 52.4% ± 0.9% (n = 24 wells). (**b**) Frequency distribution of fluorescence change (in %). Cells were bathed initially in NaCl, and the change in fluorescence was measured upon solution exchange to either NaI alone (gray, n = 1,033) or NaI + 1 mM glycine (black, n = 1,000). The ''% fluorescence change'' is defined as ((F_{final}/F_{init}) − 1) × 100 where F_{init} and F_{final} are the initial and final values of fluorescence, respectively. Averaged ''% fluorescence changes'' for the control and test experiment shown here were −5.8% ± 0.2% and −40.2% ± 0.6%. The dashed line at −20% represents a cut-off, which was manually applied to quantify coexpression efficiency of YFP and GlyRs (see Fig. 4). This cut-off identified 13.9% of cells as nonresponding. Cells were pooled from two wells each, all from the same transfection.

F_{final} are the initial and final values of fluorescence, respectively. This experiment demonstrated that the imaging system provides a robust assay of GlyR activation.

While the conventional imaging system permitted the analysis of individual cells and provided results based on hundreds of cells, larger sample sizes could be achieved using flow cytometry. To detect whether NaI + 1 mM glycine induced a change in YFP fluorescence measurable using flow cytometry, we split HEK293 cells transfected with both YFP-I152L and the GlyR α1 subunit into two tubes after harvesting the cells from culture. To the first tube, we added NaI and analyzed the cells on the flow cytometer. To the second, we added NaI + 1 mM glycine and analyzed the cells immediately. We collected ~10^4 events from each tube to quantify the YFP fluorescence. Change in YFP expression was determined by measuring mean fluorescence intensity (MFI) of cells in the presence of a control solution (NaI) or the agonist solution (NaI + glycine) and typical results are illustrated in Figure 2. YFP-positive cells treated with NaI + 1 mM glycine had lower MFI for YFP (MFI = 17,663) than cells treated with NaI alone (MFI = 35,194). These data suggested that flow cytometry could quantify changes in YFP fluorescence in response to the addition of NaI + 1 mM glycine.

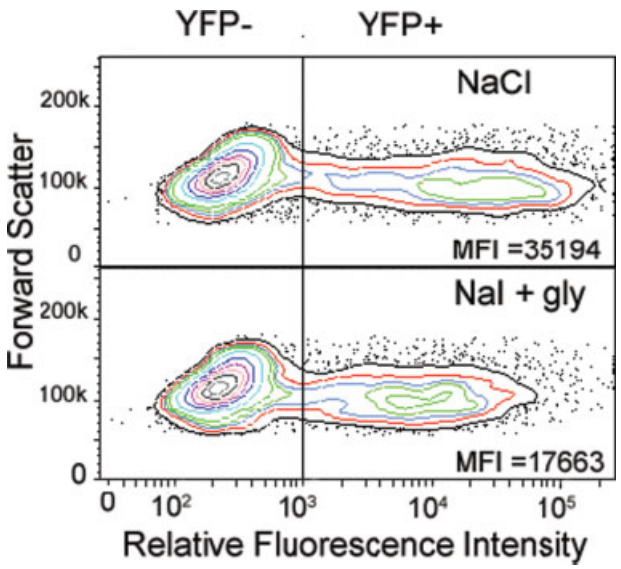

Figure 2. Contour plot of YFP relative fluorescence intensity quenching in response to agonist as measured by flow cytometry. After exclusion of cellular debris and cell clumps, a marker is positioned at the highest value of intrinsic fluorescence of YFP-negative cells. Cells with fluorescence levels above this marker are considered YFP-positive and cell numbers and levels of fluorescence recorded. Results are expressed as mean fluorescence intensities (MFI) for only YFP-positive cells and show in the upper panel YFP fluorescence intensity NaCl ''control'' compared to NaCl + NaI + glycine ''test'' treated. In this typical example there is a 50.1% decrease in MFI of YFP expressing cells post treatment, while the YFP-negative population shows no fluorescence shift.

Sensitivity of Both Assays to Graded Changes in GlyR Activity

We next transfected cells with one of 10 different GlyR constructs that were selected on the basis that their respective

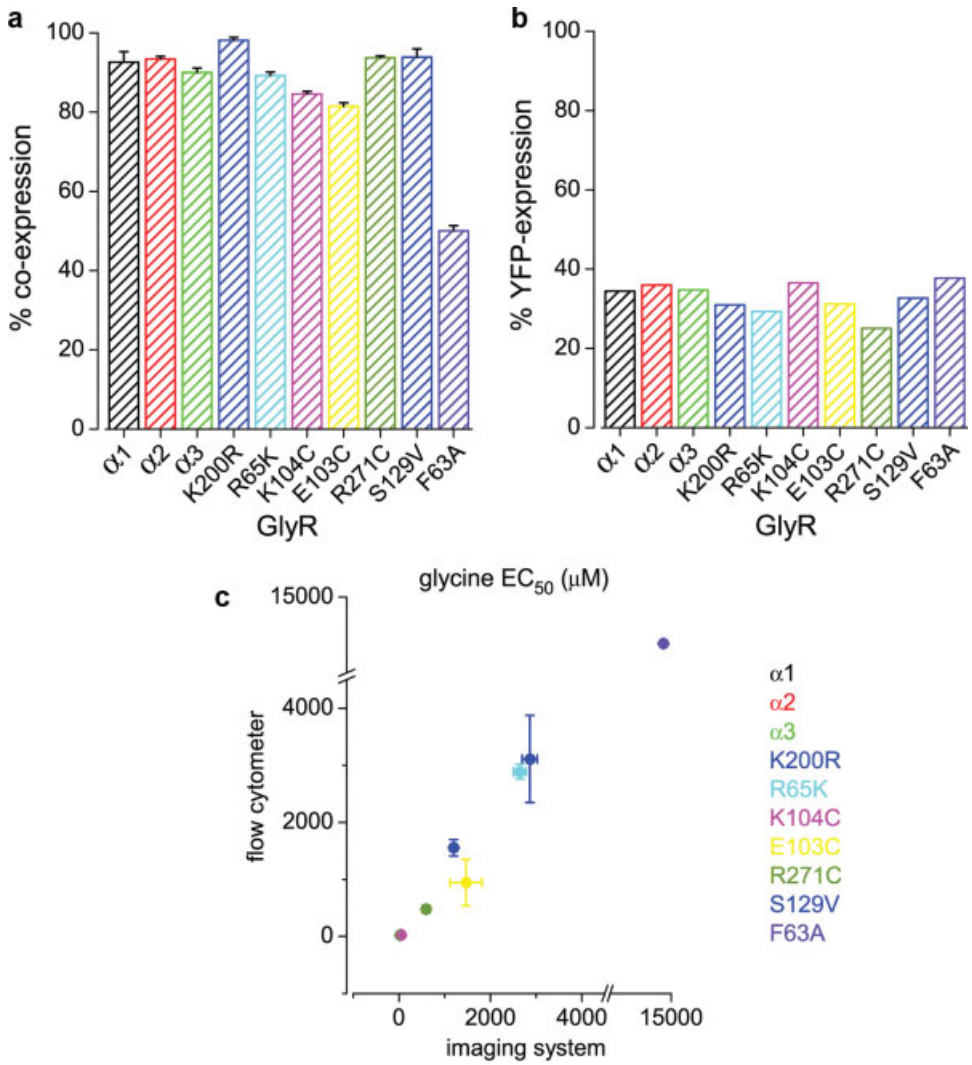

Figure 3. Quantification and correlation of YFP-I152L-expression and coexpression of YFP and GlyRs. (**a**) % YFP-expression as determined by flow cytometry. YFP-positive cells were gated based on YFP-negative controls and expressed as a percentage of live cells as determined by forward and side scattered light. (**b**) The mean percentage of YFP-expressing cells that responded with a fluorescence change of greater than −20% upon addition of NaI + 30 mM glycine using the conventional imaging system. The low value for F63A is due to the 30 mM glycine concentration being subsaturating. (**c**) Correlation analysis of glycine EC_{50}s obtained from conventional imaging and flow cytometry with nonmultiplexed cells as summarized in Table 1. Adherent cells were preincubated in NaCl control solution and activation of GlyRs was imaged 8 s after injection of NaI test solution and increasing concentrations of glycine. Suspended cells were bathed in NaCl control solution and glycine-receptor activation was induced by adding NaI test solution containing glycine in increasing concentrations. The cells were analyzed immediately (within 10 s) on the flow cytometer. Fluorescence intensities were averaged for each tested glycine concentration from $\sim 1 \times 10^4$ recorded cells. EC_{50}s were extracted from dose-response curves as stated in the text. For both experiments, cells from the same transfections were used.

glycine affinities spanned a wide range (11–14). The ultimate aim of this was to use the differing glycine sensitivities as a means of validating whether GlyR populations segregated on the basis of fluorescence multiplex decoding were functionally distinct. However, it was first necessary to determine whether both assays were consistent in their response to graded glycine concentration changes at each mutant. One feature of the conventional imaging system is that fluorescence from a single cell is recorded both before and after treatment. This feature can be used to determine the percentage of fluorescent cells that express each GlyR mutant. This was quantified by applying a saturating glycine concentration (NaI + 30 mM glycine) to cells expressing one of the 10 different GlyR constructs, and pooling results from two wells expressing the same GlyR construct. The number of cells showing a fluorescence decrease of greater than 20% was expressed as a percentage of the total number of YFP-expressing cells in the imaged wells (Fig. 3a). Virtually all YFP-expressing cells also expressed the mutant GlyRs. The low value for the F63A construct is due to a dramatically reduced glycine-sensitivity compared to the other GlyRs employed here and shows that for this receptor variant a glycine concentration of 30 mM is not saturating (13). Thus, using the conventional imaging system, we were able to confirm the coexpression of YFP with each GlyR. An identical

approach using flow cytometry is not possible as each cell is analyzed once then discarded and results are generated based on the population as a whole. Conversely, flow cytometry can be used to measure the transfection efficiency of YFP (and a given GlyR by approximation) as YFP-negative cells were also recorded, while the conventional imaging system only measures cells that are YFP positive. Transfection efficiency for each GlyR construct (Fig. 3b) was calculated using data generated during the dose-response experiment described below (Table 1). Separately, these measurements each provide a measure of the efficiency of the transfection process.

To compare the ability of both assays to report small, graded changes in GlyR activity, we assessed the concentration response for all 10 GlyR constructs using both assays. With the conventional imaging system, a single glycine concentration was applied to each well. Concentration-response relationships were constructed by pooling results from two wells exposed to the same glycine concentration so that each point on a single dose-response curve was averaged from 800 to 1200 cells. These experiments were replicated at least three times on cells transfected on different days. Curve fits to individual concentration-response relations were performed as described in materials and methods. Averaged glycine EC_{50} and n_H values of best fit are summarized in Table 1 and plotted in Figure 3c. In flow cytometry experiments, each transfection was analyzed in a separate tube using the approach described for Figure 2. Suspended cells were bathed in NaCl control solution and GlyR activation was induced by adding NaI test solution containing glycine in increasing concentrations. The cells were analyzed immediately (within 10 s) on the flow cytometer. Fluorescence intensities were averaged for each tested glycine concentration from $\sim 10^4$ recorded cells and plotted against glycine concentrations. Averaged parameters of best fit to the concentration-response curves for each GlyR construct are summarized in Table 1. None of the EC_{50} or n_H values shown in Table 1 differed significantly from one assay relative to the other ($P < 0.05$). Thus, both methods provide consistent readouts of GlyR activation status. The large variation in n_H values may reflect the fact that many of the mutants disrupt the receptor gating mechanism (6,7).

Multiplex Decoding of Cell Populations with Different Functional Properties

Having shown that data generated by both methods are comparable, we sought to increase the throughput of samples by flow cytometry. Additionally, we wanted to ensure that each group of cells was exposed to the identical concentration of agonist at the same time post-preparation. To do this, cells expressing each of the various constructs were labeled with a unique combination of cell-permeant fluorochromes, a method known as multiplexing. We chose commercially available dyes that were, capable of crossing the membrane of a live cell, being retained inside the cell and did not prevent measurement of YFP. These conditions were met by the Celltrace products produced by Molecular Probes described in Materials and Methods.

This multiplex coding (Fig. 4a) provides unique positional information about the source of the cells when different cell populations are combined. Once labeled, the cell populations were mixed together, then divided into a control solution (NaI) tube and an agonist solution (NaI + 1 mM glycine) tube. Both tubes were analyzed, the control solution tube to quantify the percentage of cells expressing YFP and their level of expression, and the agonist solution tube to quantify the change in YFP expression in response to agonist. Decoding gating is shown in Figure 4b. Fluorescence intensity of YFP-positive cells after exposure to control and agonist solutions is illustrated in Figure 4c. This typical example of three experiments illustrates the dynamic response of eight differently transfected mixed cell populations simultaneously exposed to the same agonist. The positional information was decoded using FCS Express software (De Novo Software, USA). Where more than eight cell populations were tested, the remaining cell populations were analyzed in additional multiplexed tubes, or dye combinations allowing twelve populations of cells to be multiplexed (not shown). Of the dyes used, only calcein violet was detectable in the YFP filter. To ensure that calcein violet, or any other dye, did not contribute to YFP measurements, a YFP gate was created for each population in a given multiplex. YFP gating for each mutant was based on each multiplexed population before the addition of the agonist (data not shown). These data suggest that changes in YFP fluorescence in multiplexed cells after exposure to agonist solution were measurable by flow cytometry.

We next compared the data collected using the conventional imaging system to the data collected from the decoded multiplexed cells. Ten populations of cells were used in these experiments, with each population expressing one of the 10 GlyR constructs described earlier. By titration, we found that DDAO could be used to stain two discrete populations (data not shown), increasing the total number of populations that could be multiplexed to 12. Subsequent experiments were repeated four times using 12 population multiplexing. The percentage of responding cells (treated with NaI + 1 mM glycine) measured using the conventional imaging system (assessed as for Fig. 1) was compared to the overall change in fluorescence in YFP-positive cells as measured by flow cytometry after multiplex decoding (Fig. 5a). The increased range of responses for flow cytometry data for some GlyR mutants directly reflects the larger dynamic range of this platform and longer sampling time used for flow cytometry experiments. Following addition of 1 mM Gly, the fluorescence quench in cells expressing α1 GlyRs did not vary with time (Fig. 5b), although cells transfected with α1-F63A GlyRs displayed a time-dependent quench (Fig. 5c). This difference was due to glycine sensitivity differences: the F63A mutant is weakly activated by 1 mM Gly and hence long activation times are necessary to produce significant internal Cl^- accumulation. Together, these data demonstrate comparable results from the imaging system or decoded multiplexed cells analyzed by flow cytometry.

Discussion

Flow cytometry can make quantitative (18) optical measurements of multiple fluorochromes simultaneously (19). We utilized these multiparametric capabilities to decode fluores-

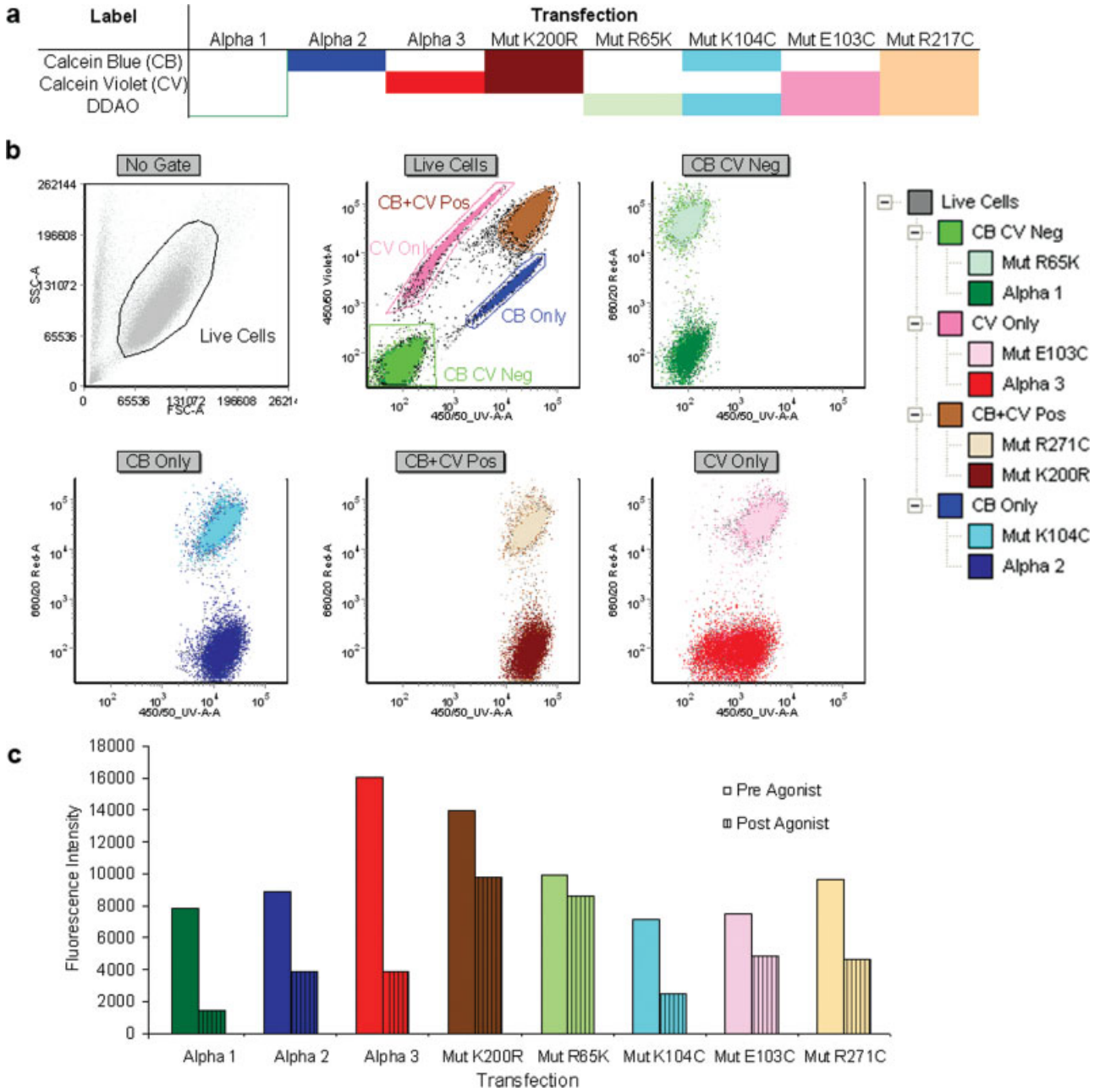

Figure 4. Resolving cell populations in multiplexed cells. Each transfected population of cells was labeled with a unique combination of cell permeant fluorophores (**a**). The gating strategy (**b**) starts with a live cell gate (top left then clockwise) from which four daughter gates are drawn based on calcein blue and calcein violet discrimination. Events contained in each of the four gates are then presented in the following plots allowing final level of decoding of events based on DDAO detection. The gate view shows the hierarchy of individual gates. MFI of YFP-positive events specific to each transfection (**c**) as determined by the gating in (b) is shown in the presence of NaI only (pre agonist) and in the presence of NaI and 1 mM glycine (post agonist).

cently labeled live HEK293 cells to measure changes in YFP fluorescence caused by Cl^- influx through GlyRs with differing glycine sensitivities. We first demonstrated that this method was capable of functionally discriminating between cells which exhibit a wide range of responses to agonist (Figs. 1 and 2). Furthermore, the glycine EC_{50} values produced by this method were similar to those resulting from conventional fluorescence microscopy of adherent cells (Table 1). These results also provide the first demonstration that the Cl^--sensitive YFP assay functions as efficiently with flow cytometry as it does with conventional microscopy.

Transfected cells expressing YFP were analyzed and the number of cells and their level of expression measured by both methods (Fig. 3). The flow cytometry approach provides rapid

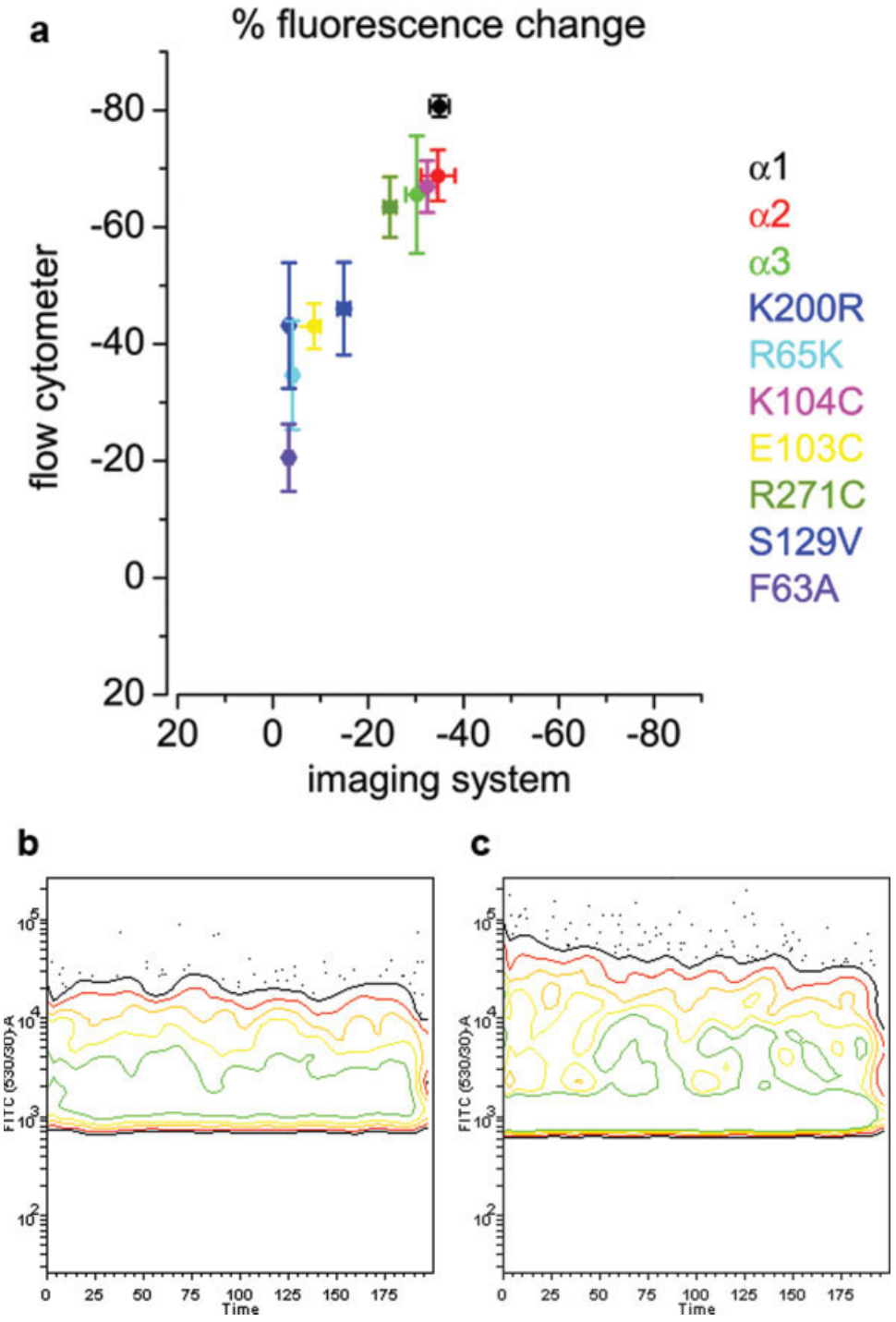

Figure 5. Comparison of fluorescence responses for conventional imaging with analysis of multiplexed cells using flow cytometry. (**a**) Correlation analysis of conventional imaging to analysis of multiplexed cells using flow cytometry. Cells were preincubated in NaCl control solution and activation of GlyRs was imaged after application of NaI test solution + 1 mM glycine. All results were averaged from four different experiments, with cells from different passages transfected on different days. (**b** and **c**) Contour plots of sample time versus change in YFP fluorescence intensity for cells expressing α1 GlyRs (b) and α1-F63A GlyRs (c). The later population accumulate Cl^- at a slow rate because of their low glycine sensitivity.

quantification of the transfection efficiency and robust statistics due to large cell numbers, as well as allowing the number of counts to be increased if the percentage of YFP-expressing cells in the total population is low. In a microscope plate-based assay, should the transfection efficiency be low, a well or experiment may be abandoned due to limited cell numbers. Multi-

plexing and pooling samples provides conditions where each cell is exposed to the same concentration of test compound and time elapsed post sample preparation. Using a plate-based method, cells may remain in the plate for various periods of time depending on well position before exposure to test compounds. As a result, cells may sit for periods of more than 30 min post-preparation at physiological temperatures before experimentation, thus paving the way for possible variability in cellular responses.

There are numerous references regarding multiplexed fluorescence assays for flow cytometry. These include methods that rely on, the binding of antibodies or antibody-coated fluorescently encoded microspheres (2) to their appropriate target, molecular interactions (20,21) and amine reactive labeling of fixed cells (5). An issue with bead/antibody encoding in live cell assays is that the act of encoding the cell, via the binding of an antibody to its ligand, may trigger intracellular events (22–24). These events may in turn alter the ability of the cell to respond to the test compound. The method described in Krutzik and Nolan et al. requires fixed and permeabilized cells (5), thereby preventing further experimentation. Our approach addressed this issue by directly labeling the cells of interest with fluorochromes which are transported into and bound within the cell (25), facilitating further experimentation on multiplexed cells. Using this approach, fluorescence has been measurable after up to seven divisions with no effect on cell viability (24–26). Here we used cell-permeant fluorochromes to label live cells and suggest that multiplexing of live cells is not restricted to this type of labeling, however, as we were assessing changes in a cell surface receptor, we chose not to use lipophilic dyes or a cell surface antibody-based multiplexing method. Our data (Fig. 4b) show that this approach yields 8–12 cell populations which are spectrally discrete in multidimensional space, while recent reports describe only the use of two populations (3,4). These populations can be decoded using standard flow cytometry analysis software and are used in this instance to provide positional information related to the coding of the cell population and its associated receptor mutation.

In summary, we have described a method for multiplexing live cells to simultaneously investigate the functional properties of multiple mutant GlyRs. This assay was specifically designed for screening libraries of random mutant GlyRs to identify the binding sites for compounds of therapeutic interest. However, the multiplexing technique as described here has other potential applications. Of course, this multiplexing method should also be equally suited to any receptor type that produces an intracellular change detectable by a fluorescent indicator, such as calcium flux measurement in the functional assessment of gamma-amino-butyric acid (GABA) receptors (26). Importantly, our experiments provide proof of principle that flow cytometry can be used for high-throughput screening of structurally related $GABA_A$ Cl^- channel receptors ($GABA_A$Rs), which are a major therapeutic target for indications including muscle relaxation, epilepsy, anxiolysis, sedation, and anesthesia (27). Indeed, the assay may be particularly applicable to the $GABA_A$R because of its extremely wide range of subunit stoichiometries. As these receptors are constructed from a family of around 19 different subunits (α1-6, β1-3, γ1-3, δ, ε, π, τ, ρ1-3), and assuming that they recombine randomly, they can theoretically produce an enormous number of receptors (>100,000), each with a distinct electrophysiological and pharmacological profile (28–30). Although the most abundant $GABA_A$Rs have trimeric $\alpha\beta\gamma$ stoichiometries, it can be difficult to reliably express all three subunits in individual cells. Our approach suggests that it should be feasible to cotransfect different subunits in IRES-containing plasmid vectors that also contain cDNAs for different genetically encoded fluorochromes. Following flow cytometry of multiplexed cells, it should be possible to distinguish cell populations expressing particular subunit combinations so that the effects of drugs (or other) treatments on individual receptor isoforms can be separately quantified.

Acknowledgments

JWL is supported by a National Health and Medical Research Council Research Fellowship.

Literature Cited

1. Sklar LA, Carter MB, Edwards BS. Flow cytometry for drug discovery, receptor pharmacology and high-throughput screening. Curr Opin Pharmacol 2007;7:527–534.
2. Fulton RJ, McDade RL, Smith PL, Kienker LJ, Kettman JR Jr. Advanced multiplexed analysis with the FlowMetrixTM system. Clin Chem 1997;43:1749–1756.
3. Young SM, Bologa CM, Fara D, Bryant BK, Strouse JJ, Arterburn JB, Ye RD, Oprea TI, Prossnitz ER, Sklar LA, Edwards BS. Duplex high-throughput flow cytometry screen identifies two novel formylpeptide receptor family probes. Cytometry A 2009; 75A: in press. DOI: 10.1002/cyto.a.20645.
4. Strouse JJ, Young SM, Mitchell HD, Ye RD, Prossnitz ER, Sklar LA, Edwards BS. A novel fluorescent cross-reactive formylpeptide receptor/formylpeptide receptor-like 1 hexapeptide ligand. Cytometry A 2009; 75A: in press. DOI: 10.1002/cyto.a.20670.
5. Krutzik PO, Nolan GP. Fluorescent cell barcoding in flow cytometry allows high-throughput drug screening and signaling profiling. Nat Methods 2006;3:361–368.
6. Legendre P. The glycinergic inhibitory synapse. Cell Mol Life Sci 2001;58:760–793.
7. Lynch JW. Molecular structure and function of the glycine receptor chloride channel. Physiol Rev 2004;84:1051–1095.
8. Harvey RJ, Depner UB, Wassle H, Ahmadi S, Heindl C, Reinold H, Smart TG, Harvey K, Schutz B, Abo-Salem OM, Zimmer A, Poisbeau P, Welzl H, Wolfer DP, Betz H, Zeilhofer HU, Müller U. GlyR alpha3: An essential target for spinal PGE2-mediated inflammatory pain sensitization. Science 2004;304:884–887.
9. Lynch JW, Callister RJ. Glycine receptors: A new therapeutic target in pain pathways. Curr Opin Investig Drugs 2006;7:48–53.
10. Zeilhofer HU. The glycinergic control of spinal pain processing. Cell Mol Life Sci 2005;62:2027–2035.
11. Galietta LJ, Haggie PM, Verkman AS. Green fluorescent protein-based halide indicators with improved chloride and iodide affinities. FEBS Lett 2001;499:220–224.
12. Kruger W, Gilbert D, Hawthorne R, Hryciw DH, Frings S, Poronnik P, Lynch JW. A yellow fluorescent protein-based assay for high-throughput screening of glycine and GABAA receptor chloride channels. Neurosci Lett 2005;380:340–345.
13. Grudzinska J, Schemm R, Haeger S, Nicke A, Schmalzing G, Betz H, Laube B. The beta subunit determines the ligand binding properties of synaptic glycine receptors. Neuron 2005;45:727–739.
14. Han NL, Haddrill JL, Lynch JW. Characterization of a glycine receptor domain that controls the binding and gating mechanisms of the beta-amino acid agonist, taurine. J Neurochem 2001;79:636–647.
15. Lynch JW, Han NL, Haddrill J, Pierce KD, Schofield PR. The surface accessibility of the glycine receptor M2-M3 loop is increased in the channel open state. J Neurosci 2001;21:2589–2599.
16. Yang Z, Ney A, Cromer BA, Ng HL, Parker MW, Lynch JW. Tropisetron modulation of the glycine receptor: Femtomolar potentiation and a molecular determinant of inhibition. J Neurochem 2007;100:758–769.
17. Chen CA, Okayama H. Calcium phosphate-mediated gene transfer: A highly efficient transfection system for stably transforming cells with plasmid DNA. Biotechniques 1988;6:632–638.
18. Schwartz A, Marti GE, Poon R, Gratama JW, Fernandez-Repolle E. Standardizing flow cytometry: A classification system of fluorescence standards used for flow cytometry. Cytometry 1998;33:106–114.
19. Perfetto SP, Chattopadhyay PK, Roederer M. Seventeen-colour flow cytometry: Unravelling the immune system. Nat Rev Immunol 2004;4:648–655.
20. Nolan JP, Lauer S, Prossnitz ER, Sklar LA. Flow cytometry: A versatile tool for all phases of drug discovery. Drug Discov Today 1999;4:173–180.
21. Perez OD, Nolan GP. Simultaneous measurement of multiple active kinase states using polychromatic flow cytometry. Nat Biotechnol 2002;20:155–162.

22. Hirsch R, Eckhaus M, Auchincloss H Jr, Sachs DH, Bluestone JA. Effects of in vivo administration of anti-T3 monoclonal antibody on T cell function in mice. I. Immunosuppression of transplantation responses. J Immunol 1988;140:3766–3772.
23. Hirsch R, Gress RE, Pluznik DH, Eckhaus M, Bluestone JA. Effects of in vivo administration of anti-CD3 monoclonal antibody on T cell function in mice. II. In vivo activation of T cells. J Immunol 1989;142:737–743.
24. Moretta A, Ciccone E, Pantaleo G, Tambussi G, Bottino C, Melioli G, Mingari MC, Moretta L. Surface molecules involved in the activation and regulation of T or natural killer lymphocytes in humans. Immunol Rev 1989;111:145–175.
25. Weston SA, Parish CR. New fluorescent dyes for lymphocyte migration studies. Analysis by flow cytometry and fluorescence microscopy. J Immunol Methods 1990;133:87–97.
26. Cui M, Chung FZ, Donahue CJ. Development of a robust GABA(B) calcium signaling cell line using beta-lactamase technology and sorting. Cytometry A 2008; 73A:761–766.
27. Mohler H, Crestani F, Rudolph U. GABA(A)-receptor subtypes: A new pharmacology. Curr Opin Pharmacol 2001;1:22–25.
28. Rudolph U, Crestani F, Mohler H. GABA(A) receptor subtypes: Dissecting their pharmacological functions. Trends Pharmacol Sci 2001;22:188–194.
29. Sieghart W, Sperk G. Subunit composition, distribution and function of GABA(A) receptor subtypes. Curr Top Med Chem 2002;2:795–816.
30. Wafford KA, Macaulay AJ, Fradley R, O'Meara GF, Reynolds DS, Rosahl TW. Differentiating the role of gamma-aminobutyric acid type A (GABAA) receptor subtypes. Biochem Soc Trans 2004;32 (Part 3):553–556.